

# Directional Adhesive Structures for Controlled Climbing on Smooth Vertical Surfaces

Daniel Santos, Sangbae Kim, Matthew Spenko, Aaron Parness, Mark Cutkosky  
Center for Design Research  
Stanford University  
Stanford, CA 94305-2232, USA  
contact: dsantos@stanford.edu

**Abstract**—Recent biological research suggests that reliable, agile climbing on smooth vertical surfaces requires controllable adhesion. In nature, geckos control adhesion by properly loading the compliant adhesive structures on their toes. These strongly anisotropic dry adhesive structures produce large frictional and adhesive forces when subjected to certain force/motion trajectories. Smooth detachment is obtained by simply reversing these trajectories. Each toe’s hierarchical structure facilitates intimate conformation to the climbing surface resulting in a balanced stress distribution across the entire adhesive area. By controlling the internal forces among feet, the gecko can achieve the loading conditions necessary to generate the desired amount of adhesion. The same principles have been applied to the design and manufacture of feet for a climbing robot. The manufacturing process of these Directional Polymer Stalks is detailed along with test results comparing them to conventional adhesives.

## I. INTRODUCTION

As mobile robots extend their range of traversable terrain, interest in mobility on vertical surfaces has increased. Previous methods of climbing include using suction [18], [19], magnets [5], [29], and a vortex [28] to adhere to a variety of smooth, flat, vertical surfaces. Although these solutions have had some success on non-smooth surfaces, in general, the variety of climbable surfaces is limited. Taking cues from climbing insects, researchers have designed robots that employ large numbers of small ( $\sim 10\mu\text{m}$  tip radius) spines that cling to surface asperities [1], [22]. This approach works well for surfaces such as concrete or brick but cannot be used for smooth surfaces like glass.

Recently, robots have been demonstrated that use adhesives for climbing. Early approaches used pressure-sensitive adhesives (PSAs) to climb smooth surfaces [9], [26], while more recent approaches used elastomeric pads [8], [27]. PSAs tend to foul quickly, which prevents repeated use, and also require relatively high energy for attachment and detachment. Elastomer pads are less prone to fouling, but generate lower levels of adhesion.

In an effort to create an adhesive that does not foul over time, there has been research on “dry” or “self-cleaning” adhesives that utilize stiff materials in combination with microstructured geometries to conform to surfaces. Fig. 1 shows a range of adhesive solutions ordered in terms of feature size and effective modulus. A material is considered tacky when the effective modulus is less than 100kPa [2],

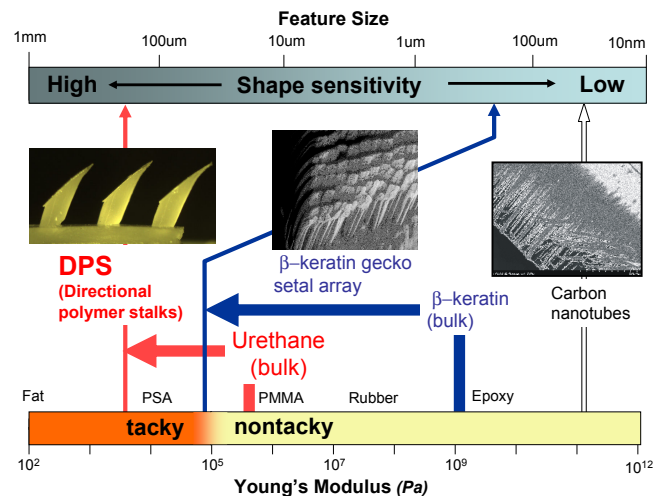


Fig. 1. Shape sensitivity of different structures and modulus of elasticity of various materials. Microstructured geometries can lower the overall stiffness of bulk materials so that they become tacky. This principle allows geckos to use  $\beta$ -keratin for their adhesive structures.

[7]. Since adhesion is primarily a result of van der Waals forces, which decrease as  $1/d^3$  where  $d$  is the distance between the materials, it is crucial to conform to the surface over all relevant length scales.

Dry adhesives, such as the gecko hierarchy of microstructures consisting of lamellae, setae, and spatulae, conform to the surface despite having bulk material stiffnesses that are relatively high (approximately 2GPa for  $\beta$ -keratin) [2]. The hierarchical geometry lowers the effective stiffness to make the system function like a tacky material.

Synthetic dry adhesives have been under development for several years. Examples include arrays of vertically oriented multiwall carbon nanotubes [31], [32] and polymer fibers [11], [15], [20], [25]. These adhesives employ stiff, hydrophobic materials and therefore have the potential to be self-cleaning. In a number of cases, useful levels of adhesion have been obtained, but only with careful surface preparation and high preloads. As the performance of these synthetic arrays improves, their effective stiffnesses could approach the 100kPa “tack criterion”.

A different approach uses structured arrays of moderately soft elastomeric materials with a bulk stiffness less than

3MPa. Because these materials are softer to begin with, they conform to surfaces using feature sizes on the order of  $100\mu\text{m}$ . One example is a microstructured elastomeric tape [8], [21]. Because the material is not very stiff, it attracts dirt. However, in contrast to PSAs, it can be cleaned and reused. The microstructured adhesive patches described in Section III, termed Directional Polymer Stalks (DPS), also employ an elastomer but are designed to exhibit adhesion only when loaded in a particular direction.

In addition to stiffness, feature size and shape of the structure is important in creating adhesion. As discussed in [10], [11], [16], [30], the available adhesive force is a function of the shape and loading of the micro-structured elements. The importance of optimizing tip shape increases as feature size increases. For extremely small elements such as carbon nanotubes, the distal geometry is relatively unimportant, but for larger features ( $O(100\mu\text{m})$ ) tip geometry drastically affects adhesion. At these sizes, the optimal tip geometry, where stress is uniformly distributed along the contact area, has a theoretical pulloff force of more than 50-100 times [10] that of a poor tip geometry. In Section III we describe the processes we have developed to obtain desired shapes at the smallest sizes our current manufacturing procedures allow, and in Section IV we present experimental results obtained with these shapes.

## II. ANISOTROPIC VERSUS ISOTROPIC ADHESION

At present, no synthetic solution has replicated the adhesion properties of gecko feet. However the main obstacle to robust climbing is not *more* adhesion but *controllable* adhesion. Sticky tape is sufficiently adhesive for a light-weight climbing robot, but its adhesive forces are difficult to control. Geckos control their adhesion with *anisotropic* microstructures, consisting of arrays of setal stalks with spatular tips. Instead of applying high normal preloads, geckos increase their maximum adhesion by increasing tangential force, pulling from the distal toward the proximal ends of their toes [3]. In conjunction with their hierarchical structures, this provides geckos with a coefficient of adhesion,  $\mu' = F_a/F_p$ , between 8 and 16 [2] depending on conditions, where  $F_a$  is the maximum normal pulloff force and  $F_p$  is the maximum normal preload force.

### A. Description of Contact Models

The frictional-adhesion model (Fig. 2) is used to describe the gecko adhesion system [3]. When pulling along the adhesive direction (B, positive tangential), the maximum adhesive force is directly proportional to the applied tangential force:

$$-F_N \leq F_T \tan \alpha^* \quad (1)$$

where  $F_N$  is the normal force,  $F_T$  is the tangential force (positive when pulling from distal to proximal), and  $\alpha^*$  is the angle of a best fit line for test data obtained with individual setae, setal arrays, and gecko toes [3]. When pulling against the adhesive direction (A), the behavior is described by Coulomb friction. An upper limit is placed on the maximum

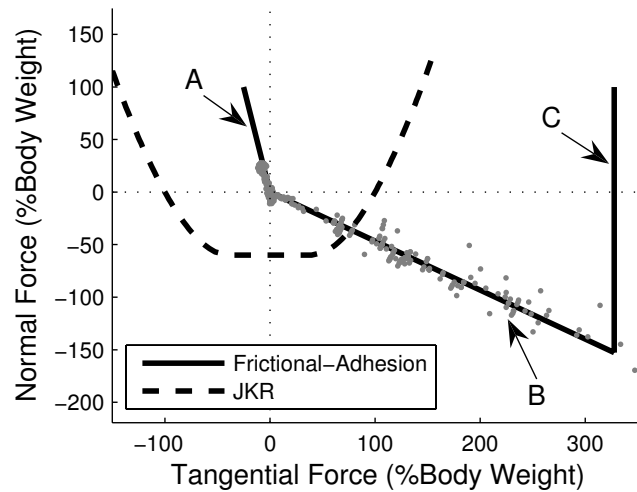


Fig. 2. Comparison of frictional-adhesion and JKR contact models. Both models have been scaled to allow a 50g gecko or robot to cling to an inverted surface. Parameters and overlaid data for the anisotropic frictional-adhesion model are from [3] for gecko setae, setal arrays, and toes. The isotropic JKR model is based on parameters in [21], [23].

tangential force in the adhesive direction (C), which is a function of limb and material strength.

Fig. 2 also compares frictional-adhesion and the Johnson-Kendall-Roberts (JKR) model [12], [13], an isotropic adhesion model based on spherical elastic asperities in contact with a flat substrate. This model predicts that maximum adhesion occurs at zero tangential force. Increasing tangential force decreases the contact area, thereby decreasing the overall adhesion. For positive values of normal force  $F_T \propto F_N^{2/3}$  [24]. The models have been scaled to give comparable values of adhesion and tangential force limits, and the curves represent the maximum normal and tangential force at which a contact will fail.

The anisotropic model shows how maximum adhesion can be controlled simply by modulating the tangential force at the contact. Its intersection with the origin allows for contact termination with negligible forces, whereas the isotropic model, which does not intersect the origin, predicts large force discontinuities at contact termination. This feature makes the anisotropic model better-suited for vertical climbing than the isotropic model. If the anisotropy is aligned properly, then gravity passively loads the contact to increase adhesion.

### B. Implications for control of contact forces

In general, both anisotropic and isotropic adhesives may provide adhesion comparable to the body weight of a gecko or a robot; however, the models lead to different approaches for controlling contact forces during climbing. A simplified planar model of a climbing gecko or robot (Fig. 3) is used for studying the implications of different contact models. Work in dexterous manipulation [14] is adapted to study the static stability of the model on inclined surfaces. There are four unknowns and three equilibrium constraints, leaving one degree of freedom: the balance of tangential force between the front ( $F_{T1}$ ) and rear ( $F_{T2}$ ) foot (i.e. the internal force),

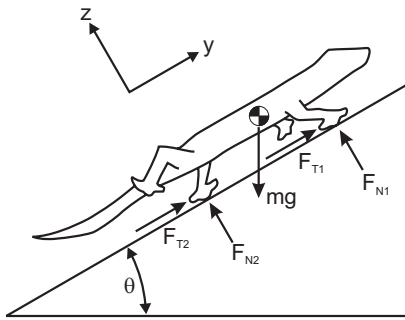


Fig. 3. 2-Dimensional model of a gecko with two feet in contact with a flat inclined plane. Foot-substrate interactions are modeled as point contacts.

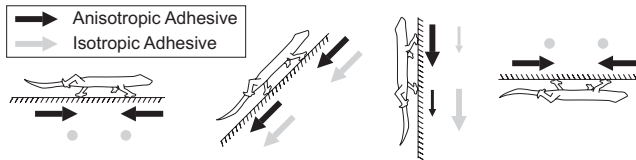


Fig. 4. Schematic of optimal tangential forces for isotropic and anisotropic adhesion at different inclinations. Arrow directions and magnitudes shown in proportion to optimal tangential forces (dot represents zero tangential force).

$F_{Int} = F_{T1} - F_{T2}$ . The maximum tangential force for each foot is limited by the contact model.

The stability of the system can be used to determine how best to distribute contact forces between the feet. The stability margin is the minimum distance, in force-space, over all feet, that any foot is from violating the contact constraints. It defines the maximum perturbation force that the system can withstand without failure of any foot contacts.

Let  $\mathbf{F}_i = [F_{T_i}, F_{N_i}]$  be the contact force at the  $i^{th}$  foot. The contact model can be defined by a parametric convex curve  $\mathbf{R}(x, y)$ , with points  $\mathbf{F} = [F_T, F_N]$  lying inside the curve being stable contacts. The distance any particular foot is from violating a contact constraint is then:

$$d_i = \min_{x,y} (||\mathbf{F}_i - \mathbf{R}(x, y)||). \quad (2)$$

For a model with two feet in contact with the surface, the overall stability margin becomes  $d = \min(d_1, d_2)$ , where  $d_1$  represents the front foot and  $d_2$  represents the rear foot.

The 2-D model's extra degree of freedom can be used to maximize the stability margin. This produces different force control strategies using the anisotropic or isotropic models at different surface inclines (Fig. 4). On a vertical surface the front foot must generate adhesion. The anisotropic model predicts the front foot should bear more of the gravity load, since increasing tangential force increases available adhesion. The isotropic model predicts the opposite, namely that the rear foot should bear more of the gravity load, because tangential forces on the front foot decrease its available adhesion. On an inverted surface, the isotropic model predicts zero tangential forces for maximum stability since gravity is pulling along the normal. Alternatively, the anisotropic model cannot generate adhesion without tangential forces and this model must rotate the rear foot and pull inward to

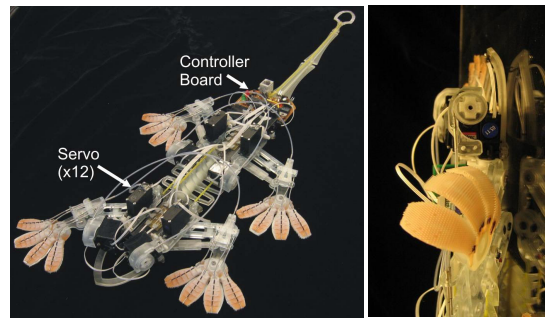


Fig. 5. Stickybot experimental climbing robot for testing directional adhesives. Each limb has two trajectory degrees of freedom (fore-aft and in-out of the wall) and one toe-peeling degree of freedom. The entire robot weighs 370 grams.

generate tangential forces that will produce enough adhesion for stability. Interestingly, the anisotropic model predicts that reversing the rear foot and pulling inward is also optimal on level ground, which would increase the maximum perturbation force that could be withstood. The predictions of the anisotropic model qualitatively match observations of geckos running on walls and ceilings and reorienting their feet as they climb in different directions [4].

### III. DESIGN AND MANUFACTURING OF ANISOTROPIC ADHESIVE PADS

The utility of anisotropic adhesion has been demonstrated on a new experimental robot, Stickybot (Fig. 5). Details of Stickybot design and control are covered in a companion paper [17]. In this section we explain the DPS manufacturing process, and in the next section we present test results comparing the DPS to isotropic stalks of equivalent size and density.

The anisotropic stalks used on the bottom of Stickybot's feet are fabricated from a polyurethane (Innovative Polymers, IE-20 AH Polyurethane, Shore-20A hardness,  $E \approx 300\text{kPa}$ ). Custom miniature tooling was used to create a mold from which the DPS were fabricated (Fig. 6). After a process of trial and error, a geometry was found that produced reasonable results for climbing. The stalks are cylindrical and tilted with respect to the backing. The upper stalk is cropped at an oblique angle that creates a sharp tip. The cylinders are  $380\mu\text{m}$  in diameter and approximately 1.0mm long from base to tip. Cylinder axes are inclined  $20^\circ$  and slanted tips are inclined  $45^\circ$ , both with respect to the vertical. The shape of the stalks is defined by the intersections of slanted circular holes with narrow Vee-shaped grooves. First, the grooves are cut into the mold using a custom  $45^\circ$  degree slitting saw. This angle dictates the angle of the tip. Slanted circular holes are then drilled into the grooves such that the opening resides entirely on the  $45^\circ$  face.

A silicone (TAP Plastics, Silicone RTV Fast Cure Mold-Making Compound) form-fitting cap is molded from the Vee grooves before holes are created. Liquid polymer is poured into the mold and capillary action fills the holes. The form-fitting cap is pressed down into the grooves, forcing excess polymer out the sides (Fig. 6). An SEM photo of

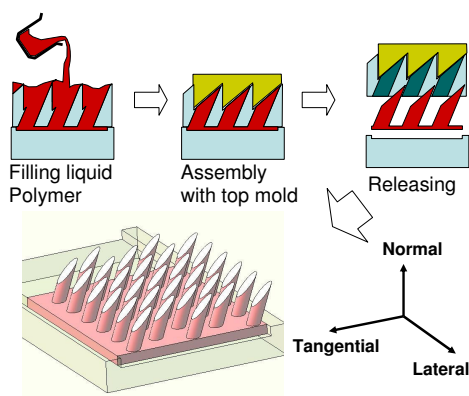


Fig. 6. Molding process used to fabricate anisotropic patches. Mold is manufactured out of hard wax and then filled with liquid urethane polymer. A cap eliminates contact with air and creates final tip geometry.

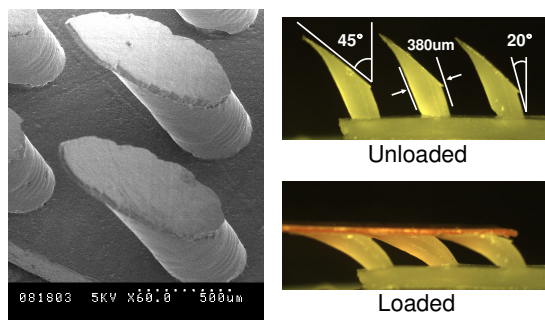


Fig. 7.  $380\mu\text{m}\phi$  anisotropic stalks oriented at  $20^\circ$  with stalk faces oriented at  $45^\circ$ , both with respect to normal.

the stalks created using this process is shown in Fig. 7. The process yields a sharp, thin tip ( $10 - 30\mu\text{m}$  thickness). When the stalks first contact a surface, this tip adheres and the tangential force required to engage the remaining area of the DPS face is very low. Fig. 7 shows the geometry of the stalks in both the unloaded and loaded states.

#### IV. ADHESION TESTS AND RESULTS

Specimens of the anisotropic material were tested under a variety of tangential and normal loading conditions to characterize their adhesive properties. For comparison, an array of isotropic cylinders (vertical cylinders of the same diameter with flat tops) made from the same polymer was also tested.

Both the anisotropic and isotropic patches were approximately elliptical in shape with a total area of  $3.5 - 4\text{cm}^2$ , corresponding to one toe of Stickybot. The anisotropic specimens contained  $\sim 500$  individual stalks while isotropic specimens contained  $\sim 250$  stalks. Specimens were prepared by washing with soap and water and then blowing dry with compressed air. They were mounted using thin double-sided tape to a flat aluminum backing.

The specimens and aluminum backing were fixed on a two-axis linear positioning stage (Velmex MAXY4009W2-S4) driven under servo control at 1kHz. Specimens were brought into contact with a stationary glass plate affixed to a

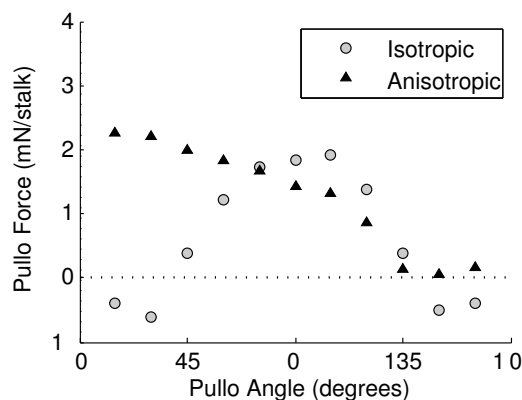


Fig. 8. Adhesion forces as a function of pulloff angle for anisotropic ( $700\mu\text{m}$  preload) and isotropic ( $150\mu\text{m}$  preload) patches. For anisotropic patches, adhesion is maximum at shallow pulloff angles in the adhesive direction and drops steadily as the angle becomes normal to the surface, becoming negligible at shallow angles in the non-adhesive direction.

6-axis force/torque sensor (ATI Gamma Transducer). The positioning stage is a stiff, screw driven device with a trajectory accuracy of approximately  $\pm 20\mu\text{m}$  while in motion at speeds of  $1\text{mm/s}$ . The sensor resolution is approximately  $25\text{mN}$  and  $0.5\text{mNm}$  for forces and torques, respectively. Force and torque data were sampled at  $1\text{kHz}$  and filtered at  $10\text{Hz}$  using a 3<sup>rd</sup> - order Butterworth filter.

Following a procedure used to measure gecko setal array adhesion forces [3], synthetic patches were moved along a controlled trajectory in the normal and tangential directions while measuring resulting forces. Specimens were brought into contact with the glass substrate and preloaded to a specified depth in the normal axis. The approach angle for the anisotropic patches was  $45^\circ$ , moving with the stalk angle (i.e. loading the stalks in the preferred direction for adhesion), and for the isotropic patch was  $90^\circ$ , along the normal direction. The patches were then pulled away from the glass substrate at departure angles between  $15^\circ$  (mostly parallel to the surface, with the angle of the anisotropic stalks) and  $165^\circ$  (mostly parallel to the surface, against the angle of the anisotropic stalks). Velocity was maintained at  $1\text{mm/s}$ , which provided a favorable tradeoff between avoiding dynamic forces and minimizing viscoelastic effects.

Fig. 8 illustrates the performance of the stalks as a function of pulloff angle. The anisotropic patches produce maximum adhesion when loaded in the positive tangential direction, as a robot would load them when clinging to a vertical wall. At angles less than  $30^\circ$ , the maximum adhesion force is approximately  $2.3\text{mN/stalk}$  ( $1.2\text{N}$  for the entire patch), and the corresponding value of  $\mu'$  was approximately 4.5. Pulling off in the normal direction generates adhesion of about  $2/3$  the peak value, and when pulling off against the angle of the stalks the adhesion drops to less than 10% the peak value. The work required to load an unload and adhesive material (Work of Adhesion) has also been used as a measure of adhesion performance [6]. At a preload of  $700\mu\text{m}$ , the maximum work loop is approximately  $5.2\text{J/m}^2$  at a  $15^\circ$  pulloff angle and the minimum work loop is  $0.3\text{J/m}^2$  at

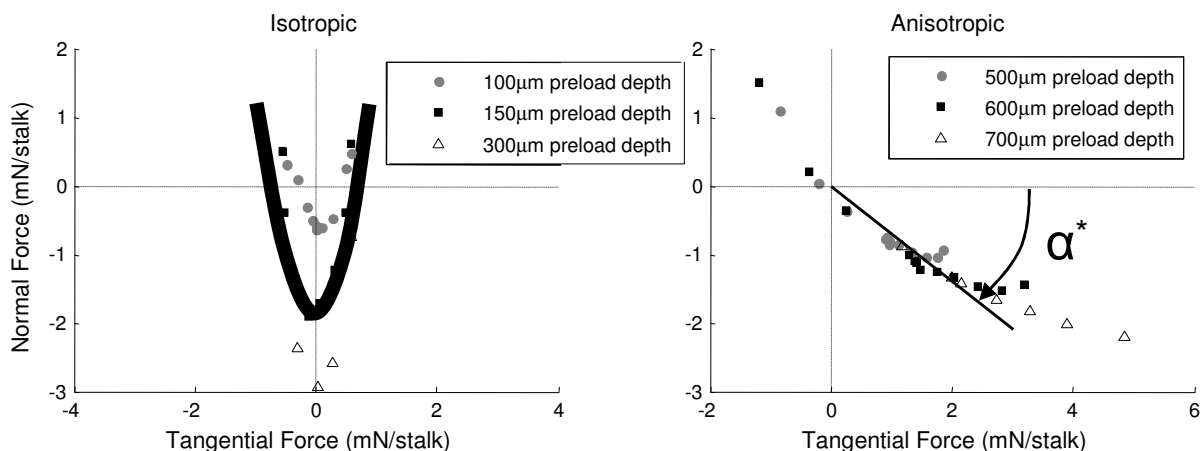


Fig. 9. Experimental limit curves for isotropic and anisotropic patches at different preload depths. Data points correspond to maximum forces at pulloff. Three series have been plotted to show the dependence of limit curves on the preload.

a  $120^\circ$  pulloff angle. For the isotropic patch, maximum adhesion is obtained when pulling off in the purely normal direction, dropping to zero for pulloff angles slightly over  $45^\circ$  with respect to the normal. The isotropic patch has a maximum adhesive force nearly as high as the anisotropic patches, but requires a higher preload force, resulting in a  $\mu'$  of approximately 0.5.

The anisotropic patches were also tested on machined granite to determine how surface roughness affects adhesion. The surface roughness ( $R_a$ ) of glass is typically less than  $10\text{nm}$  and the surface roughness of the granite is about  $10\mu\text{m}$ . At a preload depth of  $700\mu\text{m}$ , maximum adhesion force on polished granite is  $1.0\text{mN/stalk}$  ( $0.5\text{N}$  for the entire patch) resulting in an approximately 60% decrease in adhesion force compared to glass.

Fig. 9 summarizes the results for the maximum tangential and normal forces of the different patches over a range of preload depths and pulloff angles. The results can be compared directly with the models in Fig. 2. As expected, the isotropic specimen shows a behavior similar to that predicted by the JKR model: The limit curve is symmetric about the vertical axis. Maximum adhesion is obtained when pulling in the purely normal direction. Under positive normal forces Coulomb friction is observed.

The anisotropic patches behave similarly to gecko setae. Fitting a line to the data for positive values of tangential force results in an  $\alpha^* \approx 35^\circ$  (compared to approximately  $30^\circ$  for the gecko [3]). When loaded against their preferred direction ( $F_T < 0$ ) they exhibit a moderate coefficient of friction; between these two modes, the data intersects the origin. Thus, like the gecko setae, the synthetic patches can easily be detached by controlling internal forces to reduce the tangential force at the contact. However, unlike the gecko setae, the synthetic stalks start to lose adhesion at high levels of tangential force, at which point the contact faces of the stalks start to slip.

Fig. 9 also shows that forces for isotropic and anisotropic patches scale with increasing preload. For the isotropic patches, maximum adhesion is obtained when the specimen

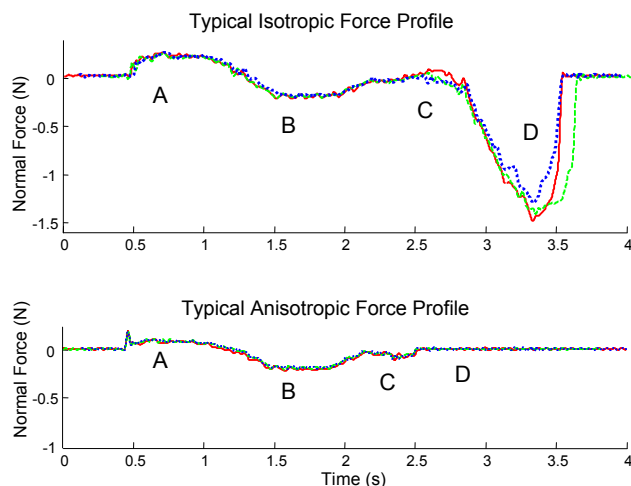


Fig. 10. Comparison of normal force profiles of anisotropic and isotropic patches on a climbing robot. Point A on the curves refers to the preloading phase of the cycle. Point B highlights when the foot is in the adhesive regime during a stroke. Points C and D are when the foot is unloaded and detached, causing large normal forces in the case of the isotropic patch.

is preloaded to  $\sim 300\mu\text{m}$  after initial contact, resulting in a normal preload of  $\sim 14.3\text{mN/stalk}$ . For the anisotropic patches, a  $700\mu\text{m}$  preload depth provided maximum adhesion, which corresponds to a preload of  $\sim 0.5\text{mN/stalk}$ . Larger preloads resulted in no further significant increase in adhesion; smaller preloads produced less adhesion.

Given the foregoing results, anisotropic and isotropic specimens can be expected to produce rather different effects when used on a robot. Fig. 10 shows typical force plots for anisotropic and isotropic toe patches on the Stickybot robot. The data for three successive cycles are plotted to show overall variability. In each case, the robot cycled a single leg through an attach/load/detach cycle on the same 6-axis force sensor in the previous tests now mounted into a vertical wall. The other three limbs remained attached to the wall throughout the experiment. In this test, the isotropic patches consisted of vertical cylinders with a thin upper membrane

bridging the gaps between the cylinders, which increased the contact area. In each case, leg trajectories were tuned empirically to provide best results for either the isotropic or anisotropic patches.

As the plots show, the isotropic patches required a larger normal force (A) to produce comparable amounts of combined tangential force and adhesion for climbing (B). The unloading step for the anisotropic patches (C, D) is accomplished rapidly and results in negligible detachment force as the leg is removed. In contrast, the isotropic patch requires a longer peeling phase (C) and produces a large pulloff force (D) as the leg is withdrawn. This large detachment force was the main limitation of the isotropic patches, producing large disturbances that frequently caused the other feet to slip.

## V. CONCLUSIONS AND FUTURE WORK

This paper describes the design and manufacture of novel adhesives and presents experimental evidence that emphasizes the importance of controllable, directional adhesion for a climbing robot. A model of gecko adhesion is presented and compared to a commonly used isotropic model from the literature, the JKR model. It is shown that the anisotropic nature of the frictional-adhesion model, combined with the fact that at zero tangential force there is zero adhesive force, allows a robot to smoothly load and unload a foot. Current work entails scaling down the size of the anisotropic stalks in order to utilize harder materials and climb rougher surfaces. This will allow for feet that are easier to clean, yet still conform and adhere well to surfaces. Future work includes using analytical or numerical methods to understand how the patch geometry will affect adhesion performance on different surfaces and extending our understanding of anisotropic adhesion to 3D. This may better predict and explain the behavior of geckos and guide the design and control of climbing robots.

## ACKNOWLEDGMENT

We thank Kellar Autumn and his students for discussions on anisotropic adhesion and testing procedure. This work was supported through the DARPA BioDynamics Program, the Intelligence Community Postdoctoral Fellow Program, and the Stanford-NIH Biotechnology Training Grant.

## REFERENCES

- [1] A. Asbeck, S. Kim, M. Cutkosky, W. Provancher, and M. Lanzetta. Scaling hard vertical surfaces with compliant microspine arrays. *International Journal of Robotics Research*, 2006.
- [2] K. Autumn. *Biological Adhesives*, volume XVII. Springer-Verlag, Berlin Heidelberg, 2006.
- [3] K. Autumn, A. Dittmore, D. Santos, M. Spenko, and M. Cutkosky. Frictional adhesion: a new angle on gecko attachment. *J Exp Biol*, 209(18):3569–3579, 2006.
- [4] K. Autumn, S. T. Hsieh, D. M. Dudek, J. Chen, C. Chitaphan, and R. J. Full. Dynamics of geckos running vertically. *J Exp Biol*, 209(2):260–272, 2006.
- [5] C. Balaguer, A. Gimenez, J. Pastor, V. Padron, and C. Abderrahim. A climbing autonomous robot for inspection applications in 3d complex environments. *Robotica*, 18(3):287–297, 2000.
- [6] A.J. Crosby, M. Hageman, and A. Duncan. Controlling polymer adhesion with “pancakes”. *Langmuir*, 21(25):11738–11743, 2005.
- [7] C.A. Dahlquist. Pressure-sensitive adhesives. In R.L. Patrick, editor, *Treatise on Adhesion and Adhesives*, volume 2, pages 219–260. Dekker, New York, 1969.
- [8] K. Daltorio, S. Gorb, A. Peressadko, A. Horschler, R. Ritzmann, and R. Quinn. A robot that climbs walls using micro-structured polymer feet. In *CLAWAR*, 2005.
- [9] K. Daltorio, A. Horschler, S. Gorb, R. Ritzmann, and R. Quinn. A small wall-walking robot with compliant, adhesive feet. In *International Conference on Intelligent Robots and Systems*, 2005.
- [10] H. Gao, X. Wang, H. Yao, S. Gorb, and E. Arzt. Mechanics of hierarchical adhesion structures of geckos. *Mechanics of Materials*, 37:275–285, 2005.
- [11] S. Gorb, M. Varenberg, A. Peressadko, and J. Tuma. Biomimetic mushroom-shaped fibrillar adhesive microstructure. *Journal of The Royal Society Interface*, 2006.
- [12] K.L. Johnson. Adhesion and friction between a smooth elastic spherical asperity and a plane surface. *Proc. of the Royal Society A: Mathematical, Physical and Engineering Sciences*, 453(1956):163–179, 1997.
- [13] K.L. Johnson, K. Kendall, and A.D. Roberts. Surface energy and the contact of elastic solids. *Proc. of the Royal Society A: Mathematical, Physical and Engineering Sciences*, 324(1558):301–313, 1971.
- [14] J. Kerr and B. Roth. Analysis of multifingered hands. *The International Journal of Robotics Research*, 4(4):3–17, 1986.
- [15] D.S. Kim, H.S. Lee, J. Lee, S. Kim, K-H Lee, W. Moon, and T.H. Kwon. Replication of high-aspect-ratio nanopillar array for biomimetic gecko foot-hair prototype by uv nano embossing with anodic aluminum oxide mold. *Microsystem Technologies*, 2006.
- [16] S. Kim and M. Sitti. Biologically inspired polymer microfibers with spatulate tips as repeatable fibrillar adhesives. *Applied Physics Letters*, 89(261911), 2006.
- [17] S. Kim, M. Spenko, and M. Cutkosky. Whole body adhesion: hierarchical, directional and distributed control of adhesive forces for a climbing robot. In *IEEE ICRA*, Rome, Italy, 2007. Accepted.
- [18] G. La Rosa, M. Messina, G. Muscato, and R. Sinatra. A lowcost lightweight climbing robot for the inspection of vertical surfaces. *Mechatronics*, 12(1):71–96, 2002.
- [19] R. Lal Tummala, R. Mukherjee, N. Xi, D. Aslam, H. Dulimarta, J. Xiao, M. Minor, and G. Dang. Development of a tracked climbing robot. *Journal of Intelligent and Robotic Systems*, 9(4), 2002.
- [20] M. Northen and K. Turner. A batch fabricated biomimetic dry adhesive. *Nanotechnology*, 16:1159–1166, 2005.
- [21] A. Peressadko and S.N. Gorb. When less is more: experimental evidence for tenacity enhancement by division of contact area. *Journal of Adhesion*, 80(4):247–261, 2004.
- [22] R. Saunders, D. Goldman, R. Full, and M. Buehler. The rise climbing robot: body and leg design. In *SPIE Unmanned Systems Technology VII*, volume 6230, Orlando, FL, 2006.
- [23] A.R. Savkoor and G.A.D. Briggs. The effect of tangential force on the contact of elastic solids in adhesion. *Proc. of the Royal Society A: Mathematical, Physical and Engineering Sciences*, 356(1684):103–114, 1977.
- [24] A. Schallamach. The load dependence of rubber friction. *Proceedings of the Physical Society. Section B*, 65(9):657–661, 1952.
- [25] M. Sitti and R. Fearing. Synthetic gecko foot-hair micro/nano-structures as dry adhesives. *Adhesion Science and Technology*, 17(8):1055, 2003.
- [26] O. Unver, M. Murphy, and M. Sitti. Geckobot and waalbot: Small-scale wall climbing robots. In *AIAA 5th Aviation, Technology, Integration, and Operations Conference*, 2005.
- [27] O. Unver, A. Uneri, A. Aydemir, and M. Sitti. Geckobot: a gecko inspired climbing robot using elastomer adhesives. In *IEEE ICRA*, pages 2329–2335, Orlando, FL, 2006.
- [28] vortex. [www.vortexhc.com](http://www.vortexhc.com), 2006.
- [29] Z. Xu and P. Ma. A wall-climbing robot for labeling scale of oil tank’s volume. *Robotica*, 20(2):203–207, 2002.
- [30] H. Yao and H. Gao. Mechanics of robust and releasable adhesino in biology: Bottom-up designed hierarchical structures of gecko. *Journal of the mechanics and physics of solids*, 54:1120–1146, 2006.
- [31] B. Yurdumakan, R. Raravikar, P. Ajayanb, and A. Dhinojwala. Synthetic gecko foot-hairs from multiwalled carbon nanotubes. *Chemical Communications*, 2005.
- [32] Y. Zhao, T. Tong, L. Delzeit, A. Kashani, M. Meyyapan, and A. Majumdar. Interfacial energy and strength of multiwalled-carbon-nanotube-based dry adhesive. *Vacuum Science and Technology B*, 2006.